

Accepted Article

Title: Post-synthetic modification of a dinuclear spin crossover iron(III) complex

Authors: Yuki Komatsumaru, Manabu Nakaya, Fumiya Kobayashi, Ryo Ohtani, Masaaki Nakamura, Leonard Lindoy, and Shinya Hayami

This manuscript has been accepted after peer review and appears as an Accepted Article online prior to editing, proofing, and formal publication of the final Version of Record (VoR). This work is currently citable by using the Digital Object Identifier (DOI) given below. The VoR will be published online in Early View as soon as possible and may be different to this Accepted Article as a result of editing. Readers should obtain the VoR from the journal website shown below when it is published to ensure accuracy of information. The authors are responsible for the content of this Accepted Article.

To be cited as: *Z. anorg. allg. Chem.* 10.1002/zaac.201800087

Link to VoR: <http://dx.doi.org/10.1002/zaac.201800087>

ARTICLE

Post-synthetic modification of a dinuclear spin crossover iron(III) complex

Yuki Komatsumaru,^[a] Manabu Nakaya,^[a] Fumiya Kobayashi,^[a] Ryo Ohtani,^[a] Masaaki Nakamura,^[a] Leonard F. Lindoy^[b] and Shinya Hayami^{*,[a],[c]}

Dedicated to Professor Peter Comba on the Occasion of his 65th Birthday

Abstract:

The dinuclear iron(III) complex [Fe(salten)₂(bipyztz)](BPh₄)₂·EtOH (**1**) was synthesized and its post-synthesis modification yielded [Fe(salten)₂(bipydz)](BPh₄)₂·EtOH (**2**). The crystal structures and magnetic behaviors of **1** and **2** were investigated by variable temperature XRD, magnetic susceptibility and Mössbauer spectra measurements, with each of these dinuclear iron(III) complexes exhibiting gradual spin crossover behavior.

Introduction

Post-synthetic modification (PSM) commonly occurs in biochemistry. For example, it occurs in the post-translational modification of proteins, whereby chemical functionality is introduced by chemical modification of an intact polypeptide.^[1] Recently, PSM has been increasingly used as a synthetic procedure for the modification of materials to produce new products that are otherwise difficult to prepare directly.^[2] In particular, PSM has proved to be a useful technique for the modification of porous materials such as silica, coordination polymers (CPs) and metal-organic-frameworks (MOFs); leading to modified frameworks that influence their gas adsorption properties.^[3] Furthermore, PSM has been used for controlling the physical properties of solid state materials, including their magnetic^[4] and photo-luminescence properties.^[5]

Spin crossover (SCO) materials exhibiting low-spin (LS) – high-spin (HS) conversion in response to external stimuli (temperature, light irradiation, pressure, and the presence of guest molecules) have been widely-investigated due to their controllable spin states.

This has allowed their potential application in molecular electronic devices.^[6] Up to now, numerous SCO compounds have been reported,^[6-13] with most of these involving a hexacoordinated iron(II), iron(III), or cobalt(II) metal environment.^[7] Over the last two decades or so, a number of MOFs exhibiting SCO behavior have been reported as well as that of numerous mono-, di-, and multi-nuclear SCO compounds.^[8] Complete, abrupt, and hysteretic spin conversions (also termed spin transitions (ST)) are now all well documented.^[9] However, the control of such behaviors remains a continuing motivation for much of the research in this area,^[10,11] with the generation of abrupt or hysteretic ST behavior being of particular interest. Ligand modification, choice of counter ion, and/or crystalizing solvent have all been employed to tune the nature of a given observed ST.^[11]

John and co-workers have investigated the SCO behavior of the MOF, [Fe(bipyztz)(Au(CN)₂)₂] (bipyztz = 3,6-bis(4-pyridyl)-1,2,4,5-tetrazine). Their focus was on the structural stability of this MOF and they were able to control the SCO behavior by converting the bipyztz linker to a bipydz (bipydz = 3,6-bis(4-pyridyl)-1,2-diazine) linker by PSM.^[12] The latter conversion involved an inverse-electron-demand, retro-Diels-Alder reaction. Since most commonly, the SCO behavior of MOFs has been tuned by the use of guest molecules,^[13] the above PSM approach represented a new strategy for controlling magnetic behavior.

In the present study, we have employed a discrete SCO complex (not a MOF) also incorporating a bipyztz ligand as a bridge between Fe(III) sites; our aim was also to control SCO behavior via structural/electronic changes produced by the PSM.

The dinuclear iron(III) complex, [Fe(salten)₂(bipyztz)](BPh₄)₂·EtOH (**1**; H₂salten = 2,2'-(iminobis(3,1-propanediyl)nitriolomethylidene))bis-phenol) was synthesized and its SCO behavior and crystal structure (Figure 1(a)) were determined. Compound **1** exhibits gradual as well as complete SCO behavior, with the nature of its ST also confirmed by variable temperature X-ray structural analysis. PSM was then performed on the bipyztz linker in **1** using the reaction illustrated in Figures 1(b) and S1. It is noted that attempts to obtain **2** from a mixture of ligand and metal source in solution were unsuccessful but it was successfully synthesized by treatment of solid **1** with 2,5-norbornadiene, followed by recrystallization of the product from acetone/EtOH. This resulted in formation of [Fe(salten)₂(bipydz)](BPh₄)₂·EtOH (**2**) which, like **1**, also showed gradual SCO behavior, with the slight difference (see later) observed for the respective spin states at 323 K also reflected in the results from their respective X-ray structural analysis.

- [a] Y. Komatsumaru, M. Nakaya, F. Kobayashi, Dr. R. Ohtani, Dr. M. Nakamura, Prof. S. Hayami
Department of Chemistry, Graduate School of Science and Technology
Kumamoto University, 2-39-1 Kurokami, Chuo-ku
Kumamoto 860-8555 (Japan)
E-mail: hayami@kumamoto-u.ac.jp
- [b] Prof. L. F. Lindoy
School of Chemistry, The University of Sydney, NSW 2006, Australia
- [c] Prof. S. Hayami
Institute of Pulsed Power Science (IPPS)
Kumamoto University, 2-39-1, Kurokami, Chuo-ku
Kumamoto 860-8555 (Japan)

ARTICLE

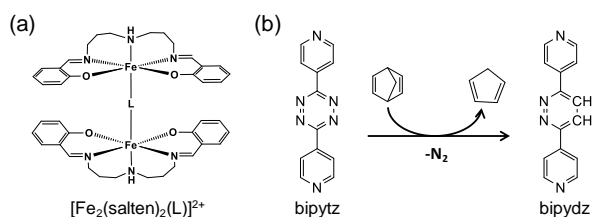


Figure 1. (a) Structure of $[\text{Fe}_2(\text{salten})_2(\text{L})]^{2+}$ (L = linker molecule) and (b) the PSM of the bipytz linker.

Results and Discussion

Single Crystal X-Ray Analysis

The structures of the dinuclear iron(III) compounds **1** and **2** were each determined at 123 and 323 K by single-crystal X-ray structural analysis (Figure 2 and Table 1), with the structural data deposited in the CCDC.^[14] Both compounds crystallized in the monoclinic space group $P2_1/c$. Each of the two iron(III) ions has an octahedral coordination geometry composed of the N_3O_2 donor atoms from a pentadentate salten ligand and an N donor from a bipytz or bipydz linker. Selected bond lengths and angles are shown in Table 1. The Fe–N and Fe–O bond lengths in **1** span the range 1.870(2)–2.013(3) Å at 123 K. The average of the Fe–N and Fe–O distances are 1.989 and 1.880, respectively; these are typical for LS iron(III) compounds incorporating a Schiff-base N_4O_2 coordination environment.^[15] At 323 K, the Fe–N and Fe–O bond lengths of **1** span the range 1.900(3)–2.139(3) Å, with the averages of the Fe–N and Fe–O distances being 2.094 and 1.970, respectively. These values are all consistent with those of a typical HS iron(III) compound incorporating a Schiff-base N_4O_2 -donor environment. The coordination bond angles are closer to a regular octahedron upon the spin transition from the HS to the LS state; both the bond lengths and angles are consistent with the occurrence of SCO behavior. In **2**, the average Fe–N and Fe–O distances are 1.873(2) and 2.013(3) at 123 K, and 1.888(4) and 2.126(5) at 323 K. The presence of a slightly larger HS domain in **1** than in **2** at 323 K was indicated by the slightly larger octahedral distortion in **1** ($\Sigma = 30.9^\circ$) around the metal center compared to **2** ($\Sigma = 29.8^\circ$). Compound **1** has the π - π interactions between BPh_4 (C27–C32) and bridging ligand (C26, N5, N6) [centroid-centroid distance = 3.641 at 123 K]. Compound **2** also has π - π interactions [centroid-centroid distance = 3.667 Å at 123 K]. Although the distances of π - π interactions are almost the same, the angles between the planes constituting the respective aromatic rings are 12.42° and 13.85°, respectively. Compound **2** has larger angles between planes due to the effect of aromatic ring distortion. Further details are listed in Table S1. The Fe–Fe distance in one molecule of the dinuclear complex **1** is 15.341 Å at 323 K and, for **2** it is 15.309 Å at this temperature (Figures S2, S3).

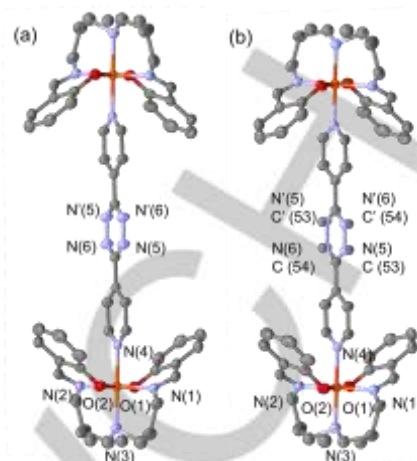


Figure 2. (a) Crystal structure of (a) **1**-EtOH and (b) **2**-EtOH. Hydrogen atoms are omitted for clarity.

Table 1. Representative bond distances and angles for **1** and **2**.

Compound	1		2	
Temperature (K)	123	323	123	323
Bond distance (Å)				
Fe–O(1)	1.890(2)	1.900(3)	1.889(2)	1.902(4)
Fe–O(2)	1.870(2)	1.914(3)	1.873(2)	1.888(4)
Fe–N(1)	1.967(3)	2.026(3)	1.968(3)	2.018(5)
Fe–N(2)	2.013(3)	2.107(4)	2.013(3)	2.099(5)
Fe–N(3)	1.957(3)	2.035(3)	1.954(3)	2.012(5)
Fe–N(4)	1.996(2)	2.139(3)	1.995(3)	2.126(5)
Bond angles (°)				
O(1)–Fe–O(2)	179.1(1)	173.7(1)	179.2(1)	173.8(2)
O(1)–Fe–N(1)	89.3(1)	88.3(1)	89.0(1)	88.0(2)
O(1)–Fe–N(2)	89.4(1)	93.2(1)	89.5(1)	92.6(2)
O(1)–Fe–N(3)	91.6(1)	91.1(1)	91.5(1)	93.3(2)
O(1)–Fe–N(4)	89.7(9)	87.2(1)	89.8(1)	86.7(2)
O(2)–Fe–N(1)	89.9(1)	93.1(1)	90.3(1)	91.0(2)
O(2)–Fe–N(2)	90.4(1)	93.0(1)	90.4(1)	93.5(2)
O(2)–Fe–N(3)	89.3(1)	88.1(1)	89.2(1)	88.2(2)
O(2)–Fe–N(4)	90.47(9)	86.6(1)	90.3(1)	87.3(2)
N(1)–Fe–N(2)	89.8(1)	87.5(1)	89.1(1)	86.9(2)
N(1)–Fe–N(3)	178.7(1)	174.9(1)	178.8(1)	175.0(2)
N(1)–Fe–N(4)	91.4(1)	91.1(1)	91.4(1)	94.2(2)
N(2)–Fe–N(3)	89.8(1)	87.4(1)	89.8(1)	88.3(2)
N(2)–Fe–N(4)	178.9(1)	178.5(1)	179.1(1)	178.6(2)
N(3)–Fe–N(4)	89.7(1)	94.0(1)	89.7(1)	90.6(2)
Σ	6.97	30.9	7.8	29.8

ARTICLE

Magnetic susceptibility

The temperature dependencies of the magnetic susceptibilities of **1** and **2** were measured in the temperature range of 5–400 K. The $\chi_m T$ vs. T plots are shown in Figure 3. Gradual one-step SCO behavior was observed in both cases. The $\chi_m T$ value for **1** was $1.19 \text{ cm}^3 \text{ K mol}^{-1}$ and for **2** it was $1.35 \text{ cm}^3 \text{ K mol}^{-1}$, both at 85 K. These values are slightly larger than expected for two uncoupled LS iron(III) ions ($0.75 \text{ cm}^3 \text{ K mol}^{-1}$, $g = 2$) and indicate the existence of HS domains. Thus the observed plateaux are consistent with the presence of both HS and LS domains below 100 K. On heating, **1** showed gradual incomplete SCO behavior with the $\chi_m T$ value increasing from $1.19 \text{ cm}^3 \text{ K mol}^{-1}$ at 85 K to $7.48 \text{ cm}^3 \text{ K mol}^{-1}$ at 400 K. Compound **2** also showed gradual incomplete SCO behavior. For this system the $\chi_m T$ value increased from $1.35 \text{ cm}^3 \text{ K mol}^{-1}$ at 85 K to $5.93 \text{ cm}^3 \text{ K mol}^{-1}$ at 400 K. These SCO behaviors reflect the presence of a mixture of HS and LS states, in accord with incomplete SCO between $S = 1/2$ and $S = 5/2$. The difference in the $\chi_m T$ values at 400 K for **1** and **2** undoubtedly reflect the influence of different structural and electronic factors. Intermolecular interactions typically cause an increase in the cooperativity between molecules leading to more abrupt SCO behavior.^[16] The presence of π - π interaction involving the bridging (pillar) ligand is perhaps one of the factors influencing cooperativity because aromatic ring distortion on transforming the tetrazine to diazine will decrease intramolecular orbital overlap and, as a consequence, tend to inhibit intermolecular π - π interactions. Cooperativities caused by intermolecular interaction are more prominent at higher temperature. This while **1** and **2** show similar magnetic susceptibilities at low temperature, they show different magnetic susceptibilities in the higher temperature region, with a steeper increase in the $\chi_m T$ value for **1**. This outcome is concordant with the bond length and bond angle data from the single crystal structure determinations discussed earlier.

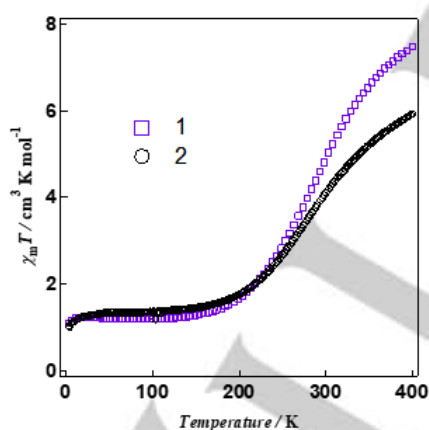


Figure 3. Variable temperature magnetic behavior for **1** and **2**.

Mössbauer Spectra

The Mössbauer spectra of **1** and **2** were each measured at three temperatures, with the results shown in Figures 4 and S4, respectively. The Mössbauer spectra each consist of two doublet peaks; shown as red and blue traces in Figure 4.

As for **1**, the doublet with isomer shift (I.S.) of 0.46 mm s^{-1} and quadrupole splitting (Q.S.) of 0.87 mm s^{-1} is assigned to the HS state

of iron(III), I.S. of 0.24 mm s^{-1} and Q.S. of 2.09 mm s^{-1} is assigned to LS state of iron(III) at 85 K. The Mössbauer data show that $\sim 17.5\%$ of the HS domain remains at this lower temperature. Similarly for **2**, two doublet peaks were observed. The doublet with I.S. of 0.44 mm s^{-1} and Q.S. of 0.82 mm s^{-1} is assigned to the HS state of iron(III), I.S. of 0.24 mm s^{-1} and Q.S. of 2.09 mm s^{-1} is assigned to the LS state of iron(III) at 85 K. As the temperature increases, the ratio of the HS state present also increases. This change in the ratio is consistent with the observed SCO magnetic susceptibility results. The value of the isomer shift decreases as the temperature increases due to the influence of the second-order Doppler shift.

Electronic spectra

The UV-Vis spectra of bipytz, bipydz as well as of **1** and **2** were measured in acetonitrile at 25°C (Figure 5a). Generally, it is known that a Diels-Alder process can be monitored directly through a color change, corresponding in the present case to the conversion of bipytz to bipydz.^[17] The spectra of bipytz and bipydz are shown in Figure 5a. In contrast to bipydz, bipytz showed the expected characteristic absorption at 550 nm arising from the $n \rightarrow \pi^*$ electronic transition being observed in the visible region due to the presence of a low-lying π^* orbital.^[18] The UV-Vis spectra of **1** and **2** are shown in Figure 5b. The spectrum of **1** exhibits absorptions at 425 nm ($\epsilon = 2675 \text{ L / mol cm}$) and 490 nm ($\epsilon = 3007 \text{ L / mol cm}$) while for **2** they occur at 425 nm ($\epsilon = 2787 \text{ L / mol cm}$) and 475 nm ($\epsilon = 3123 \text{ L / mol cm}$). These peaks are as expected for the presence of a mixture of a HS and LS domains for iron(III).^[19] In this case, we could not monitor directly the color changes between compound **1** and **2** because the weaker tetrazine $n \rightarrow \pi^*$ band substantially overlaps the more intense MLCT absorptions. However, as **1** reacts to form **2**, a decrease in absorption intensity and a shift of the main absorption peak from 490 to 475 nm is seen. It is assumed that these changes are caused by the PSM reaction as this will undoubtedly influence the electronics of the adjacent iron(III) centers. However, as might be anticipated, PXRD determinations showed that the PSM process only results in minimal changes in the observed patterns for **1** and **2** (Figure S5).

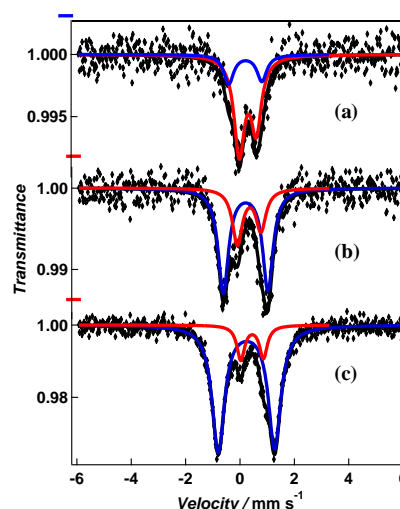


Figure 4. Mössbauer spectra for **1** at (a) 300K, (b) 250K (c) 85K.

ARTICLE

Table 2. Mössbauer parameters for 1 and 2.

Compound	T [K]		δ [mms ⁻¹]	ΔE_Q [mms ⁻¹]	$\Gamma/2$ [mms ⁻¹]	Area ratio [%]
1	85	HS(Fe ^{III})	0.4632	0.8698	0.3931	17.5
		LS(Fe ^{II})	0.2441	2.0892	0.5484	82.5
	250	HS(Fe ^{III})	0.3373	0.8662	0.4434	31.2
		LS(Fe ^{II})	0.2065	1.6397	0.4599	68.8
	300	HS(Fe ^{III})	0.2999	0.6227	0.4654	76.4
		LS(Fe ^{II})	0.2094	1.2172	0.4365	23.6
2	85	HS(Fe ^{III})	0.4513	0.7620	0.4226	24.6
		LS(Fe ^{II})	0.2465	2.1373	0.5338	75.4
	250	HS(Fe ^{III})	0.4246	0.8434	0.4221	30.6
		LS(Fe ^{II})	0.2268	1.6832	0.4876	69.4
	300	HS(Fe ^{III})	0.3031	0.8357	0.5335	64.3
		LS(Fe ^{II})	0.2243	1.4080	0.5474	35.7

[a] δ = isomer shift; ΔE_Q = quadrupole splitting; $\Gamma/2$ = half-height width of the line

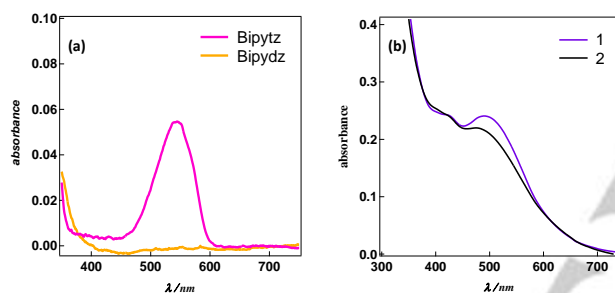


Figure 5. UV-Vis spectra for (a) bipytz and bipydz in chloroform (100 μ M), (b) 1 and 2 in acetonitrile (40 μ M).

Conclusions

The dinuclear tetraazine-containing SCO complex [Fe(salten)₂(bipyztz)](BPh₄)₂ (**1**) has been synthesized and its diazine derivative, [Fe(salten)₂(bipydz)](BPh₄)₂ (**2**), was generated by PSM. Compound **2** was not able to be obtained from a mixture of ligand and metal source in solution but could only be obtained by adding 2,5-norbornadiene to compound **1** in the solid state. Relative to compound **1**, **2** exhibits a change in its magnetic behavior that is assigned to electronic influences arising from the PSM transformation of the tetraazine-containing complex to its corresponding diazine derivative along with the resulting (small) differences in the intermolecular and intramolecular interactions that occur in these structures.

Experimental Section

Synthesis of 3,6-di(pyridine-4-yl)-1,2,4,5-tetrazine (bipyztz)

3,6-Di(pyridine-4-yl)-1,2,4,5-tetrazine was synthesized following the reported literature method.^[20] To a solution of 4-cyanopyridine (1.0 g, 10 mmol) hydrazine monohydrate (6 mL) and deionized water (1.5 mL) was added concentrated HCl (1.2 mL) dropwise. The resulting mixture was refluxed for 4 h then cooled to room temperature and the orange compound that formed was collected

by filtration. This product was dispersed in acetic acid (50 mL) and then 60% HNO₃ (10 mL) was added dropwise. The resulting purple solid was collected by filtration. Finally recrystallized from pyridine gave 0.55 mg (44%) of purple crystals. ¹H NMR (500 MHz, CDCl₃): δ = 8.46 (dd, J (H,H) = 2.9, 6.3 Hz, 2H; CH), 8.90 (dd, J (H,H) = 2.9, 6.3 Hz, 2H), ppm.

Synthesis of 3,6-bis(4-pyridyl)-1,2-diazine (bipydz)

3,6-Di(pyridine-4-yl)-pyridazine was synthesized by the reported literature method.^[15] ¹H NMR (500 MHz, CDCl₃): δ = 8.78 ppm (d, J (H,H) = 5.7 Hz, 2H; CH), 8.00 ppm (dd, J (H,H) = 4.6, 8.0 Hz, 2H; CH), ppm.

Synthesis of [Fe(salten)₂(bipyztz)](BPh₄)₂ (**1**) (H₂salten = 2,2'-[iminobis(3,1-propanediyl)nitrilomethylidene]bis-phenol)

The synthesis of **1** was based on previously reported literature method.^[21] To 3,3'-diaminodipropylamine (0.21 g, 2 mmol) in MeOH (25 mL) was added salicylaldehyde (0.49 g, 4 mmol) in MeOH (25 mL). The resulting mixture was refluxed for 2 h. then Fe(NO₃)₃ · 9H₂O (0.81 g, 2 mmol) in MeOH (10 mL) was added to the yellow solution. To the resulting dark purple solution was added bipyztz (0.13 g, 1 mmol) in MeOH (50 mL) and the mixture was refluxed for 2 h. After cooling the solution to room temperature, sodium tetraphenylborate (1.03 g, 3 mmol) in MeOH (10 mL) was added and the solution was stirred for 1 h. The purple precipitate that had formed was collected by filtration and washed with ether. Recrystallization of this product from acetone/ethanol (1:1) gave dark purple crystals. C₁₀₃H₁₀₃B₂Fe₂N₁₂O_{5.5} (1706.30): calcd. C 71.50, H 6.00, N 9.71; found C 71.70, H 6.37, N 9.89.

Synthesis of [Fe(salten)₂(bipydz)](BPh₄)₂ (**2**)

Compound **2** was prepared by heating a mixture of **1** and excess 2,5-norbornadiene to 75 °C for 17 h. After cooling the reaction mixture to room temperature, the dark purple product was washed with ether, and recrystallized from acetone/EtOH (1:1). C₁₀₂H₁₀₄B₂Fe₂N₁₀O₈ (1760.69): calcd. C 70.76, H 6.06, N 8.09; found C 70.41, H 6.04, N 8.2.

Physical Measurements.

Single-crystal X-ray data for **1** and **2** were recorded on an Oxford Gemini Ultra diffractometer employing graphite monochromated Mo K α radiation generated from a sealed tube (λ = 0.7107 Å). Data integration and reduction were undertaken with CrysAlisPro. Using Olex2, the structure was solved with the ShelXT structure solution program using Direct Methods and refined with the ShelXL refinement package using Least Squares minimization. Hydrogen atoms were included in idealized positions and refined using a riding model. Powder X-ray diffraction data (PXRD) were collected on a RIGAKU SmartLab (40 kV/30 mA) X-ray diffractometer using Cu K α radiation (λ = 1.5406 Å) in the 2θ range of 5°–30° with a step width of 1.0°. Temperature-dependent magnetic susceptibilities for **1** and **2** between 5 K and 400 K were measured using a superconducting quantum interference device (SQUID) magnetometer (Quantum Design MPMS XL) in an external field of 0.5 T. The Mössbauer spectrometer, with a ⁵⁷Co/Rh source, was operated in the transmission mode. Electronic spectra were recorded on a Shimadzu UV-3600 spectrophotometer. Elemental analyses (C, H, N) were carried out on a J-SCIENCE LAB JM10 analyser at the Instrumental Analysis Centre of Kumamoto University.

Supporting Information

ARTICLE

Crystallographic data, intermolecular distances, temperature dependence of Mössbauer spectra and Powder XRD patterns.

Acknowledgements

This work was supported by KAKENHI Grant-in-Aid for Scientific Research (A) JP17H01200.

Keywords: Iron(III), Dinuclear, Spin-crossover, Post-synthetic modification.

Reference

- [1] C. T. Walsh, S. Garneau-Tsodikova, G. J. Gatto, *Angew. Chem. Int. Ed.* **2005**, *44*, 7342–7372.
- [2] a) D.A. Roberts, B.S. Pilgrim, J.D. Cooper, T.K. Ronson, S. Zarra, J.R. Nitschke, *J. Am. Chem. Soc.* **2015**, *137*, 10068–10071. b) S. M. Cohen, *Chem. Sci.* **2010**, *1*, 32–36.
- [3] a) T. Grancha, J. Ferrando-Soria, H.-C. Zhou, J. Gascon, B. Seoane, J. Pasán, O. Fabelo, M. Julve, E. Pardo, *Angew. Chem. Int. Ed.* **2015**, *54*, 6521–6525. b) Ahnfeldt, T., Gunzelmann, D., Loiseau, T., Hirsemann, D., Senker, J. r., Ferey, G., Stock, N., *Inorg. Chem.* **2009**, *48*, 7, 3057–3064. c) S. A. Amolegbe, H. Ohmagari, K.Wakata, H.Takehira, R.Ohtani, M. Nakamura, C. Yu, S. Hayami, *J. Mater. Chem. B*, **2016**, *4*, 1040–1043.
- [4] K.S. Asha, N. Ahmed, R. Nath, D. Kuznetsov, S. Mandal, *Inorg. Chem.* **2017**, *56*, 7316–7319.
- [5] Wang, X., Feng, M., Xiao, L., Tong, A., Xiang, Y, *ACS Chem. Biol.* **2016**, *11*, 444–451.
- [6] a) Halcrow, M. A., Wiley Chichester, U.K., **2013**, *Spin-crossover Materials: Properties and Applications* b) Halcrow M. A., *Chem. Soc. Rev.* **2011**, *40*, 4119–4142. C) V. V. Novikov, I. V. Ananyev, A. A. Pavlov, M. V. Fedin, K. A. Lyssenko Y. Z. Voloshin, *J. Phys. Chem. Lett.* **2014**, *5*, 496–500.
- [7] a) S. Hayami, O. Sato, K. Inoue, Y. Einaga, Y. Maedaa, *J. Nucl. Rad. Sci.* **2002**, *3*, A1–A9. b) T. Shimizu, Y. Komatsu, H. Kamihata, Y. H. Lee, A. Fuyuhiko, S. Iijima, S. Hayami, *J. Incl. Phenom. Macrocycl. Chem.* **2011**, *71*, 363–369. c) C. A. Kilner and M. A. Halcrow, *Dalton Trans.* **2010**, *39*, 9008–9012 d) J. Cirera, V. Babin, F. Paesani, *FInorg. Chem.* **2014**, *53*, 11020–11028.
- [8] C.-F. Wang, M.-J. Sun, Q.-J. Guo, Z.-X. Cao, L.-S. Zheng and J. Tao, *Chem. Commun.* **2016**, *52*, 14322–14325.
- [9] S. Hayami, Z.-Z. Gu, H. Yoshiki, A. Fujishima, O. Sato, *J. Am. Chem. Soc.* **2001**, *123*, 11644–11650.
- [10] a) Sun, L., Zhang, S., Qiao, C., Chen, S., Yin, B., Wang, W., Wei, Q., Xie, G., Gao, S. *Inorg. Chem.* **2016**, *55*, 10587–10596. b) I.-R. Jeon, O. Jeannin, R. Clérac, M. Rouzières and M. Fourmigué, *Chem. Commun.*, **2017**, *53*, 4989.
- [11] a) Fatur, S. M., Shepard, S. G., Higgins, R. F., Shores, M. P., Damrauer, N. H., *J. Am. Chem. Soc.* **2017**, *139*, 4493–4505. b) W. Phonsri, P. Harding, L. Liu, S. G. Telfer, K. S. Murray, B. Moubaraki, T. M. Ross, G. N. L. Jameson and D. J. Harding, *Chem. Sci.* **2017**, *8*, 3949.
- [12] J.E. Clements, J.R. Price, S.M. Neville, C.J. Kepert, *Angew. Chem. Int. Ed.* **2014**, *53*, 10164–10168.
- [13] a) C.H. Pham, J. Cirera, F. Paesani, *J. Am. Chem. Soc.* **2016**, *138*, 6123–6126. b) S.S. Nagarkar, A.V. Desai, S. K. Ghosh, *Chem. Asian J.* **2014**, *9*, 2358 – 2376. b) Ohba, M., Yoneda, K., Agusti, G., Munoz, M. C., Gaspar, A. B., Real, J. A., Yamasaki, M., Ando, H., Nakao, Y., Sakaki, S., Kitagawa, S. *Angew. Chem. Int. Ed.* **2009**, *48*, 4767–4771. c) P.D. Southon, L. Liu, E.A. Fellows, D.J. Price, G.J. Halder, K.W. Chapman, B. Moubaraki, K.S. Murray, J.F. Létard, C.J. Kepert, *J. Am. Soc. Chem.* **2009**, *131*, 10998–11009.
- [14] CCDC 1827261–1827264 contain the supplementary crystallographic data for this paper. These data are provided free of charge by The Cambridge Crystallographic Data Centre.
- [15] K. Tanimura, R. Kitashima, N. Bre fuel, M. Nakamura, N. Matsumoto, S. Shova, J.-P. Tuchagues, *Bull. Chem. Soc. Jpn.* **2005**, *78*, 1279–1282.
- [16] a) Jonathan A. Kitchen, Brooker, S., *Coord. Chem. Rev.* **2008**, *252*, 2072–2092 b) Halcrow, M. A., Ed.; Wiley: Chichester, U.K., 2013. c) Banerjee, H., Chakraborty, S., Saha-Dasgupta, T., A Theoretical Overview. *Inorganics* **2017**, *5*, 47.
- [17] A.-C. Knall, M. Hollauf, C. Slugovc, *Tetrahedron Lett.* **2014**, *55*, 4763–4766. b) R. A. A. Foster and M. C. Willis, *Chem. Soc. Rev.* **2012**, *42*, 63–76.
- [18] Clavier, G., Audebert, P., *Chem. Rev.* **2010**, *110*, 3299–3314.
- [19] a) S. Hirose, S. Hayami, Y. Maeda, *Bull. Chem. Soc. Jpn.* **2000**, *73*, 2059–2066. b) S. Schenker, A. Hauser, R.M. Dyson, *Inorg. Chem.* **1996**, *35*, 4676. b) S. Hayami, K. Inoue, S. Osaki, Y. Maeda, *Chem. Lett.* **1998**, *27*, 987–988.
- [20] T.K. Pal, S. Neogi, P. K. Bharadwaj, *Chem. Eur. J.* **2015**, *21*, 16083–16090.
- [21] S. Hayami, Y. Hosokoshi, K. Inoue, Y. Einaga, O. Sato, Y. Maeda, *Bull. Chem. Soc. Jpn.* **2001**, *74*, 2361–2368.

ARTICLE

Additional Author information for the electronic version of the article.

Author: ORCID identifier
Author: ORCID identifier
Author: ORCID identifier

WILEY-VCH

Accepted Manuscript